

# Perfusion-induced redox differences in cytochrome *c* oxidase: ATR/FT-IR spectroscopy

Rebecca M. Nyquist<sup>a,b</sup>, Dirk Heitbrink<sup>a</sup>, Carsten Bolwien<sup>a</sup>, Todd A. Wells<sup>b</sup>,  
Robert B. Gennis<sup>b,c</sup>, Joachim Heberle<sup>a,\*</sup>

<sup>a</sup>Forschungszentrum Jülich, IBI-2: Biologische Strukturforchung, 52425 Jülich, Germany

<sup>b</sup>Center for Biophysics and Computational Biology, University of Illinois at Urbana-Champaign, Urbana, IL 61801, USA

<sup>c</sup>Department of Biochemistry, University of Illinois at Urbana-Champaign, Urbana, IL 61801, USA

Received 6 July 2001; accepted 27 July 2001

First published online 17 August 2001

Edited by Vladimir Skulachev

**Abstract** Attenuated total reflection (ATR) spectroscopy brings an added dimension to studies of structural changes of cytochrome *c* oxidase (CcO) because it enables the recording of reaction-induced infrared difference spectra under a wide variety of controlled conditions (e.g. pH and chemical composition), without relying on light or potentiometric changes to trigger the reaction. We have used the ATR method to record vibrational difference spectra of CcO with reduction induced by flow-exchange of the aqueous buffer. Films of CcO prepared from *Rhodobacter sphaeroides* and beef heart mitochondria by reconstitution with lipid were adhered to the internal reflection element of the ATR device and retained their full functionality as evidenced by visible spectroscopy and time-resolved vibrational spectroscopy. These results demonstrate that the technique of perfusion-induced Fourier-transform infrared difference spectroscopy can be successfully applied to a large, complex enzyme, such as CcO, with sufficient signal/noise to probe vibrational changes in individual residues of the enzyme under various conditions. © 2001 Federation of European Biochemical Societies. Published by Elsevier Science B.V. All rights reserved.

**Key words:** Vibrational spectroscopy; Lipid; Membrane protein; Respiration; Proton translocation; Electron transfer; Bacteriorhodopsin

## 1. Introduction

Cytochrome *c* oxidase (CcO) is the terminal, oxygen-reducing enzyme in the respiratory chain of mitochondria as well as many bacteria, and it efficiently catalyzes the conversion of dioxygen to water [1]. During this process it transfers four electrons from four reduced cytochrome *c* molecules, consumes four protons for the chemical conversion of each dioxygen molecule, and pumps four additional protons from the inside (mitochondrial matrix or bacterial cytoplasm) to the

outside (mitochondrial intermembrane space or bacterial periplasm). The net movement of these charges contributes to the electrochemical gradient across the membrane. Ascertaining the means by which electron transfer, proton pumping, and the oxygen chemistry are coordinated is essential to understand this molecular machine.

The core machinery of CcO includes a team of conserved amino acids, three copper atoms (two Cu<sub>A</sub> and one Cu<sub>B</sub>), and two hemes (Fe<sub>a</sub> and Fe<sub>a3</sub>), with Fe<sub>a3</sub> and Cu<sub>B</sub> forming the binuclear center, the site at which the molecular oxygen is chemically converted to water (see [2] for a recent review). Several intermediate states in the course of the catalytic cycle have been identified by visible spectroscopy, i.e. by optical absorbance changes observed when the metal centers undergo changes in valence, spin, and ligation states. During enzymatic turnover, changes at the binuclear center must be linked to protein conformational changes and to the protonation states of particular residues to control the oxygen chemistry and the proton pumping. The nature of these changes is not known.

X-ray crystallographic models at 2.3–3.5 Å exist for CcO and related quinol oxidases from several species [3–7], including *Rhodobacter sphaeroides* (Svensson-Ek et al., unpublished results). Therefore, groundwork is already in place to provide a suitable basis for designing and interpreting studies of the structural changes occurring throughout the catalytic cycle. Vibrational difference spectroscopy can be very helpful in elucidating such changes. For example, infrared vibrational difference spectroscopy has contributed towards determining the mechanism of proton pumping in bacteriorhodopsin (bR), a membrane protein in purple bacteria that converts the energy of a photon into an electrochemical gradient by pumping one proton from the cytoplasm to the extracellular region (see [8] for a recent review). In this case, detailed band assignments of the infrared difference spectra throughout the catalytic cycle have greatly contributed to an understanding of molecular details pertinent to the proton pumping mechanism.

A comprehensive assignment of the infrared spectra of CcO throughout its catalytic cycle lags far behind that of bR. This is partly due to the fact that trapping a homogeneous intermediate state is not straightforward with CcO. Whereas the catalytic cycle of bR is initiated by light, the complete cycle of CcO requires initiation by electron transfers in the presence of oxygen. Differences between the oxidized and fully-reduced forms of the enzyme have been characterized by Fourier-transform infrared (FT-IR) difference spectroscopy using electrochemical [9–12] or photoreductive techniques [13–16].

\*Corresponding author. Fax: (49)-2461-61 2020.  
E-mail address: [j.heberle@fz-juelich.de](mailto:j.heberle@fz-juelich.de) (J. Heberle).

**Abbreviations:** CcO, cytochrome *c* oxidase; bR, bacteriorhodopsin; ATR, attenuated total reflection; IRE, internal reflection element; FT-IR, Fourier-transform infrared; R<sub>4</sub>-O, fully-reduced minus oxidized; Cu<sub>A</sub>, copper A; Cu<sub>B</sub>, copper B; Fe<sub>a</sub>, iron of heme *a*; Fe<sub>a3</sub>, iron of heme *a*<sub>3</sub>

However, vibrational difference spectra of the oxygenated intermediate states of CcO have not yet been reported. One reason for this is that these intermediate states are most easily generated by altering the chemical composition of the solution. In general, it is not possible using transmission FT-IR methods to alter the solution chemical composition through perfusion while simultaneously holding the protein concentration constant.

The attenuated total reflection (ATR) method of FT-IR spectroscopy [17,18] surmounts these limitations because the enzyme is immobilized on the surface of an internal reflection element (IRE). The immobilized sample is immersed in a reservoir of buffer which can be exchanged (i.e. perfused), thereby permitting spectra of the same sample to be recorded under a variety of solution conditions. Perfusion-induced differences in the protein can, thus, be examined on a single population of protein molecules.

## 2. Materials and methods

### 2.1. Enzyme preparation

*R. sphaeroides* was grown and purified as described earlier [19]. Beef heart mitochondrial CcO was isolated and purified by standard methods [20,21].

### 2.2. Preparation of reconstituted CcO films

The reconstitution procedure required preparation of mixed vesicles of lipid and detergent. Vesicles of dimyristoylphosphatidylcholine (Sigma) were prepared by ultrasonication [22] with a buffer solution of 10 mM phosphate, pH 8, containing 2% w/v cholate (Sigma). The purified enzyme was added to the lipid-cholate vesicles at a molar protein to lipid ratio of 1:1 for bovine CcO and 5:1 for *R. sphaeroides* CcO. The volume of the solution was adjusted by adding buffer (10 mM phosphate, pH 8) to 500  $\mu$ l/mg protein, and the mixture was stirred for 30 min. at 4°C. Bio-Beads SM-2 (Bio-Rad), cleaned and equilibrated with 10 mM phosphate buffer, pH 8, were stirred into the protein-lipid solution over the course of 8 h at 4°C. A total of 1 g beads were added in portions to 500  $\mu$ l protein-lipid solution.

### 2.3. Visible spectroscopic characterization of the protein-lipid films

Films of CcO were examined by drying the protein-lipid solution onto the inner wall of a cuvette, immersing the film in oxygenated buffer containing 50 mM phosphate, 100 mM KCl, pH 8, and recording the oxidized spectrum (Shimadzu UV-2101PC UV-VIS). A reduced spectrum was then obtained after exchanging the buffer for degassed buffer containing 50 mM phosphate, 90 mM KCl, 10 mM sodium dithionite, pH 8. To return to the oxidized state, the dithionite-containing reducing solution was exchanged for the oxidizing buffer and the measurements repeated on the same film. For comparison, oxidized and reduced spectra were performed on a detergent-solubilized enzyme in 50 mM phosphate, 100 mM KCl, pH 8, 0.05% dodecylmaltoside, reduced with 10 mM dithionite.

### 2.4. Vibrational spectroscopic characterization of the protein-lipid films

All FT-IR spectra were acquired with a Bruker IFS 66v at 20°C (see [18,23] for further technical details). Films of fully-reduced CO-bound lipid-solubilized enzyme for reflection spectroscopy were prepared by drying 100  $\mu$ l of reconstituted CcO solution onto a ZnS IRE in a home-built, out-of-compartment ATR accessory [18], and immersing it in 2 ml CO-saturated 50 mM phosphate, 90 mM KCl, 10 mM sodium dithionite, pH 8. Samples of fully-reduced CO-bound detergent-solubilized enzyme for transmission measurements were prepared as previously described [16]. In both transmission and ATR measurements, the frequency-doubled 532 nm line of a Nd:YAG laser, with pulses of 10 ns duration at 40 mJ, was used to photolyse the CO. Spectra were acquired in step-scan mode with 100  $\mu$ s time resolution [18]. Resonance-Raman spectroscopy was performed on the LABRAM spectrometer from Jobin-Yvon. Reconstituted CcO was dried onto the inner wall of a quartz cuvette, immersed in buffer as described for visible spectroscopy, and probed by the 413.1 nm emission of a Kr<sup>+</sup> laser (Innova 90C, Coherent).

### 2.5. Vibrational redox difference spectroscopy

Films for ATR/FT-IR spectroscopy were created by gently drying 10  $\mu$ l of 20  $\mu$ M protein-lipid solution with a nitrogen stream onto the diamond IRE of a custom-modified ATR accessory (Applied Systems International). Resulting films were immersed in an aqueous solution of 50 mM phosphate, 100 mM KCl, pH 8, and equilibrated for at least 2 h. The oxygen-containing buffer was exchanged to a degassed reducing solution containing 50 mM phosphate, 90 mM KCl, 10 mM sodium dithionite, pH 8, and a reduced spectrum recorded. The film was then cycled back to the oxidized state with several washes of 50 mM phosphate, 100 mM KCl, pH 8, buffer. Four cycles of 5000 scans each were recorded at 2  $\text{cm}^{-1}$  resolution and averaged. Photo-reduction samples were prepared according to [16], i.e. 300  $\mu$ M detergent-solubilized CcO in 50 mM Tris buffer, 50  $\mu$ M riboflavin and 50 mM EDTA, pH 8, applied between two BaF<sub>2</sub> windows with 10  $\mu$ m pathlength. Light-activation of the flavin was accomplished by 100 pulses of the third harmonic of a Nd:YAG (355 nm) laser of 10 ns pulse duration and 10 Hz repetition, with an energy of 35 mJ/cm<sup>2</sup>/pulse. Spectra from two samples were averaged, each with 1000 scans of the reduced state rationed to 1000 scans of the unphotolysed (oxidized) state. No subtractions, corrections, or smoothing have been applied to the spectra.

## 3. Results and discussion

Adhesion of CcO to the IRE, allowing an exchange of the buffer without significant loss of protein, is essential for the feasibility of the ATR perfusion studies. Removal of the detergent used in purification and the addition of phospholipids were employed to facilitate the adhesion of CcO to the IRE surface. The procedure of Rigaud et al. [24,25] was modified with a 10 000-fold decrease in the amount of exogenous lipid per protein compared to previous CcO reconstitutions that reported using this method [26,27]. In order to maximize signals of interest, thick films as opposed to single bilayers were used to take advantage of the penetration depth of the evanescent wave that irradiates the sample (several hundred nanometers in the amide region [17]). For both maximal protein concentration and maximal adhesion to the IRE, the ratio of exogenous lipid-protein was adjusted empirically. The optimal protein-lipid ratio differed for beef heart and *R. sphaeroides* CcO, and likely depends on the endogenous lipid con-

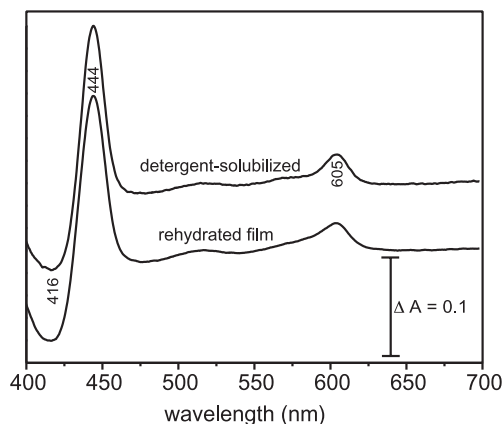


Fig. 1. R<sub>4</sub>-O absorption difference spectra of CcO from *R. sphaeroides* in the visible range. The upper curve presents the difference spectrum of detergent-solubilized enzyme, while the lower curve represents the difference spectrum of lipid-reconstituted CcO films immersed in buffer solution. Films were cycled between oxidized and fully-reduced by exchanging the bulk aqueous buffer for degassed sodium dithionite-containing buffer. The detergent-solubilized spectrum is normalized to the Soret peak of the film.

tent of the enzyme preparations as well as the particular detergent used in purification.

### 3.1. Visible spectroscopic characterization of the protein–lipid films

The films withstand the exchange of solution without decrease in concentration. This enables the comparison of visible and infrared spectra to be repeated on the same film, i.e. the same population of CcO molecules can be cycled through various states. Thus, we have examined the visible spectra under simulated conditions of the ATR/FT-IR experiments. Subtraction of the oxidized (O) visible absorption spectrum from the fully-reduced ( $R_4$ ) spectrum (i.e. the  $R_4$ –O spectrum) reveals characteristic electronic transition differences, specifically a Soret peak at 444 nm and an  $\alpha$ -peak at 605 nm [28]. Fig. 1 shows the visible  $R_4$ –O spectra for *R. sphaeroides* CcO, comparing spectra from detergent-solubilized and protein–lipid films. The band positions of detergent-solubilized and reconstituted CcO are in agreement for both the *R. sphaeroides* CcO as well as beef heart CcO (data not shown). For both species, the ratio of the Soret to  $\alpha$  peak heights for detergent-solubilized and protein–lipid films are identical. The data clearly demonstrate that the redox spectrum is not affected by the drying/rehydration process, and that full reduction and re-oxidation of the hemes take place within the films.

### 3.2. Vibrational spectroscopic characterization of the protein–lipid films

The CcO films were characterized by time-resolved infrared spectroscopy in an examination of the CO-rebinding kinetics. CO binds to the reduced  $Fe_{a3}$ , as indicated by the  $C\equiv O$  stretching vibration at  $1963\text{ cm}^{-1}$  with *R. sphaeroides* CcO or  $1964\text{ cm}^{-1}$  with bovine CcO. The  $Fe$ – $CO$  bond can be photolysed with high quantum yield [29], with rebinding of CO to  $Fe_{a3}$  on the millisecond time-scale at room temperature [30]. This characteristic time serves as a measure of the integrity of the binuclear center and its environment. Characteristic times for CO-rebinding for beef heart CcO were determined in films using the ATR technique, and comparing them to those

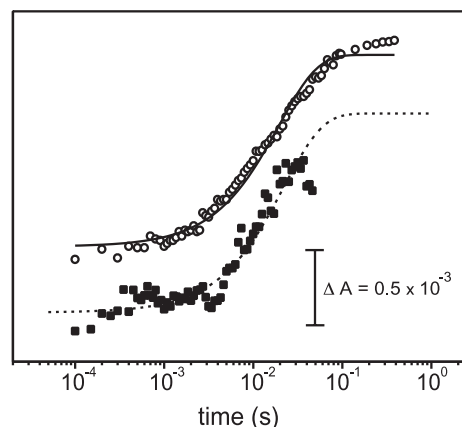


Fig. 2. Rebinding kinetics after photolysis of CO to  $Fe_{a3}$  in CcO from beef heart mitochondria. The absorbance of the  $Fe_{a3}$ -bound  $C\equiv O$  stretch at  $1963\text{ cm}^{-1}$  is followed over time after the laser flash. The open circles correspond to detergent-solubilized (transmission) data and the dark squares to protein–lipid films immersed in bulk aqueous buffer (ATR) data. The data are fit to a single exponential, shown as the solid curve (detergent-solubilized) and the dotted curve (films immersed in bulk aqueous buffer), with CO-rebinding time-constants of  $19.5 \pm 0.7\text{ ms}$  and  $22.1 \pm 1.3\text{ ms}$ , respectively. The data for detergent-solubilized samples are offset by  $0.5\text{ m O.D.}$  for clarity.

of the detergent-solubilized enzyme using transmission FT-IR spectroscopy [16]. The comparison (Fig. 2) shows close agreement of the resulting time constants:  $19.5 \pm 0.7\text{ ms}$  for the detergent-solubilized bovine CcO and  $22.1 \pm 1.3\text{ ms}$  for the films of bovine CcO. The agreement indicates that the heme-copper binuclear center of the protein is unharmed by the preparation procedure. This is corroborated by the fact that the resonance-Raman spectra of the oxidized and the fully-reduced state (data not shown) are identical to those previously described for the solubilized enzyme [31].

Experiments with polarized infrared radiation did not reveal any significant dichroism of the amide vibrations. Thus, these films apparently do not self-assemble into aligned multilayers upon drying onto the IRE in this fashion. Nonetheless,

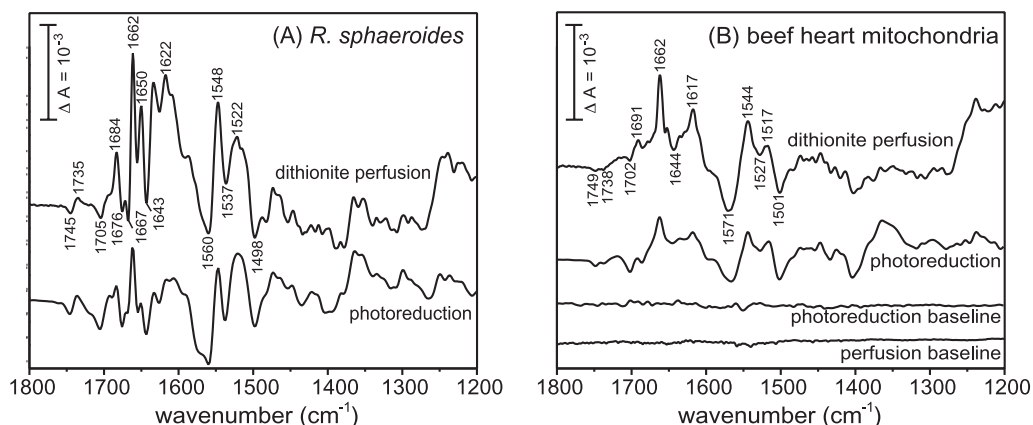


Fig. 3. Infrared  $R_4$ –O difference spectra of CcO from (A) *R. sphaeroides* and (B) beef heart mitochondria. In both panels, the upper curve shows the dithionite-perfusion spectrum of protein–lipid films, and the lower curve shows the results from photoreduction in transmission using detergent-solubilized enzyme. The two lower-most curves in panel B represent controls where difference spectra were acquired under photoreduction conditions, but in the absence of protein, and perfusion induced  $R_4$ –O difference spectra acquired in the absence of the reductant dithionite. Curves are not normalized for concentration, nor have any subtractions, corrections, or smoothing been applied. Prominent peaks are labeled, some of which are discussed in the text.

the possibility of small patches of aligned membrane stacks, with stacks arranged isotropically with respect to each other, is not ruled out.

### 3.3. FT-IR redox difference spectroscopy

For perfusion-redox ATR measurements, the pH and ionic strength of the bulk solutions were carefully matched in order to minimize the effects of swelling/shrinking of the films, which alters the concentration of protein within the evanescent wave. The spectroscopic changes observed after dithionite-induced reduction are entirely reversible upon re-oxidation, even for small features. The reversible spectra attest to the stability of the protein–lipid films for several days and throughout multiple changes of the buffer.

The redox-induced difference spectra of bacterial CcO are shown in Fig. 3A. Difference bands assigned to vibrational changes of the formyl side chain of heme  $a_3$  (C=O at  $1662\text{ cm}^{-1}$  [32]), the heme propionates (C=O at  $1676\text{ cm}^{-1}$  [11]) and glutamic acid 286 (C=O at  $1745$  (–)/ $1735$  (+)  $\text{cm}^{-1}$ ) are clearly resolved. Direct comparisons with the difference spectrum obtained by photoreduction of the detergent-solubilized enzyme reveals that the ATR method of dithionite-perfusion of the films reproduces these results. It is apparent from the inspection of the spectra of the control experiments (see the two traces at the bottom of Fig. 3B) that the difference bands of the redox-induced experiments are well above noise. Also, previously published redox-induced FT-IR difference spectra of *Paracoccus denitrificans* CcO [9] and *R. sphaeroides* CcO [13] agree well with both spectra presented in Fig. 3A. Slight deviations in band position and amplitude may arise from the different origin of the enzyme. Similarly, the features of perfusion-induced  $R_4$ –O spectrum of the beef heart CcO (Fig. 3B) concur with the electrochemically-induced redox FT-IR spectrum as well [12].

One of the most significant differences between the *R. sphaeroides* and bovine CcO FT-IR redox spectra occurs in the region between  $1780$  and  $1710\text{ cm}^{-1}$  where the C=O stretch of protonated carboxylic acids occur. The *R. sphaeroides* spectrum has a characteristic negative peak at  $1745\text{ cm}^{-1}$  and positive peak at  $1735\text{ cm}^{-1}$  (Fig. 3A), while the bovine spectrum has two negative peaks, at  $1749$  and  $1738\text{ cm}^{-1}$  (Fig. 3B). The  $1745/1735\text{ cm}^{-1}$  spectral feature has also been observed in the redox spectra of *P. denitrificans* [9] and the *Escherichia coli*  $bo_3$ -type quinol oxidase [13]. These redox peaks were further investigated with site-directed mutants [10,14,15], without clear consensus emerging from the data and interpretation. In particular, there has been ambiguity as to whether the entire feature can be ascribed to key carboxylate E286 (*R. sphaeroides* numbering), or whether another residue contributes [10].

The negative  $1745\text{ cm}^{-1}$  and positive  $1735\text{ cm}^{-1}$  peaks in the difference spectrum of CcO from *R. sphaeroides* (continuous line in the wild-type spectrum of Fig. 4) both downshift by  $6\text{ cm}^{-1}$  when measured in  $D_2O$  (broken line in Fig. 4), as expected for the C=O stretch of carboxylic acids. To definitively assign the  $1745/1735\text{ cm}^{-1}$  spectral feature, the conservative mutants E286Q and E286D of *R. sphaeroides* were employed. In the spectrum of the mutant E286Q, both the positive and negative peaks from the wild-type feature entirely disappear from the  $1780\text{ cm}^{-1}$  to  $1710\text{ cm}^{-1}$  region (middle spectrum in Fig. 4). The exchange of this glutamic acid to aspartic acid preserves the differential band shape, although

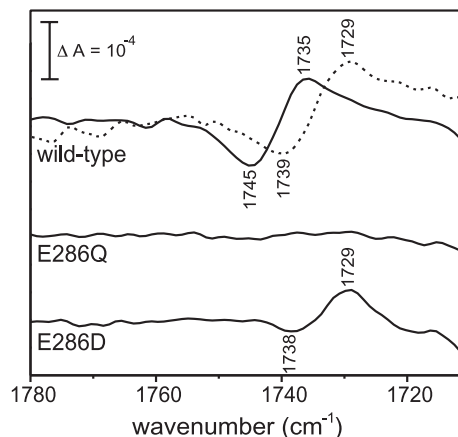


Fig. 4. Enlarged view of the perfusion-induced  $R_4$ –O difference spectra over the range  $1780$ – $1710\text{ cm}^{-1}$ . The top solid line is from wild-type *R. sphaeroides* CcO in  $H_2O$ , while the dotted line corresponds to the spectrum in  $D_2O$  buffer (pH 8). The middle spectrum represents the difference spectrum of the mutant E286Q. At the bottom, the  $R_4$ –O spectrum of the E286D mutant is displayed.

the entire feature shifts down to  $1738$  (–)/ $1729$  (+)  $\text{cm}^{-1}$  (bottom spectrum in Fig. 4). Our results contrast to those for the *P. denitrificans* CcO mutants [10] where a residual band at  $1732\text{ cm}^{-1}$  remained in both equivalent mutants. The authors concluded that the negative signal at  $1734\text{ cm}^{-1}$  of the wild-type CcO might then be caused by another Asp or Glu, not yet identified, indicating protonation of E278 (equivalent to E286 in *R. sphaeroides*) and deprotonation of the second residue upon oxidation of the protein. Also, contrary to [10], we do not find any pH dependence of the peak shape or positions of the  $1745/1735\text{ cm}^{-1}$  spectral feature over the pH range  $5.0$ – $9.5$  (data not shown).

It is evident from the data presented here that, for the *R. sphaeroides* enzyme, both  $1745$  and  $1735\text{ cm}^{-1}$  peaks arise solely from a change in the hydrogen-bonding environment of the protonated carboxylic acid moiety of E286 rather than a deprotonation upon reduction. The downshift of the frequency of the carboxylic side chain is indicative of a more strongly hydrogen-bonded E286 in the fully-reduced state. The carboxylic group of the aspartic acid in the E286D mutant undergoes a similar hydrogen-bonding alteration during the transition, but is downshifted due to different hydrogen-bond length of the shorter side chain and perhaps slight structural differences in its environment. It is not possible to discern whether the C=O bond of the glutamine in the E286Q mutant also undergoes a similar change in hydrogen bonding during the transition because the resulting negative/positive feature would be downshifted to the region around  $1700\text{ cm}^{-1}$ , where it may overlap with other stronger band features in the redox spectrum. Nonetheless, we have clearly resolved the peaks in the  $1780$ – $1710\text{ cm}^{-1}$  region of the spectrum, eliminating ambiguity surrounding the  $1745/1735\text{ cm}^{-1}$  spectral feature for the *R. sphaeroides* CcO and demonstrating the acute sensitivity of the perfusion-induced difference technique for observing structural changes of individual amino acid side chains.

## 4. Conclusions

The present work demonstrates that CcO from *R. sphae-*

roides and beef heart can be reconstituted at high protein concentrations and rehydrated into thick protein–lipid films, suitable for ATR/FT-IR measurements of perfusion-induced differences. The enzyme remains adhered and maintains high concentration after multiple exchanges of the buffer. Spectroscopic criteria as well as CO binding kinetics suggest that the protein is not adversely affected by the process and functions identically to the detergent-solubilized preparation. Most importantly, the R<sub>4</sub>–O difference spectra obtained by dithionite-perfusion using ATR are essentially the same as the redox difference spectra obtained from photoreduction as well as potentiometric titrations using transmission FT-IR spectroscopy. From a close evaluation of the FT-IR redox spectra between 1780 and 1710 cm<sup>-1</sup> for wild-type and E286 mutants of *R. sphaeroides* CcO, we have shown that the 1745/1735 cm<sup>-1</sup> spectral feature arises solely from a change in the hydrogen-bonding environment of the protonated carboxylic acid moiety of E286 rather than a deprotonation upon reduction. The perfusion-induced ATR difference technique allows vibrational difference spectra of CcO to be obtained with sensitivity at the level of individual amino acids, under a wide variety of chemical conditions, including those under which oxygenated intermediates of the catalytic cycle are stable. Future perfusion-induced ATR difference spectra of CcO should yield valuable structural insights which have not yet been possible with other FT-IR methods. Studies of other large membrane protein complexes are also possible with this technique.

**Acknowledgements:** We are grateful to M. Fabian (Rice University, Houston, TX, USA), P. Brzezinski and H. Sigurdson (University of Stockholm, Sweden) for their generous gifts of purified beef heart enzyme. We thank G. Büldt for his support and interest. In addition, J.H. expresses deepest gratitude to the late Bo Malmström for introducing him to the field of CcO during a 1 month visit to his lab. The work was supported by Grants from the NIH, HL16101 (to R.B.G.) and Training Grant 5-T32 GM08276-13 (to R.M.N.) as well as the Deutsche Forschungsgemeinschaft, SFB-189, Project C6 (to J.H.).

## References

- [1] Babcock, G.T. and Wikström, M. (1992) *Nature* 356, 301–309.
- [2] Zaslavsky, D. and Gennis, R.B. (2000) *Biochim. Biophys. Acta* 1458, 164–179.
- [3] Tsukihara, T., Aoyama, H., Yamashita, E., Tomizaki, T., Yamaguchi, H., Shinzawa-Itoh, K., Nakashima, R., Yaono, R. and Yoshikawa, S. (1995) *Science* 269, 1069–1074.
- [4] Yoshikawa, S., Shinzawa-Itoh, K., Nakashima, R., Yaono, R., Yamashita, E., Inoue, N., Yao, M., Fei, M.J., Libeu, C.P., Mizushima, T., Yamaguchi, H., Tomizaki, T. and Tsukihara, T. (1998) *Science* 280, 1723–1729.
- [5] Iwata, S., Ostermeier, C., Ludwig, B. and Michel, H. (1995) *Nature* 376, 660–669.
- [6] Abramson, J., Riistama, S., Larsson, G., Jasaitis, A., Svensson-Ek, M., Laakkonen, L., Puustinen, A., Iwata, S. and Wikström, M. (2000) *Nat. Struct. Biol.* 7, 910–917.
- [7] Soulimane, T., Buse, G., Bourenkov, G.P., Bartunik, H.D., Huber, R. and Than, M.E. (2000) *EMBO J.* 19, 1766–1776.
- [8] Heberle, J. (2000) *Biochim. Biophys. Acta* 1458, 135–147.
- [9] Hellwig, P., Rost, B., Kaiser, U., Ostermeier, C., Michel, H. and Mantele, W. (1996) *FEBS Lett.* 385, 53–57.
- [10] Hellwig, P., Behr, J., Ostermeier, C., Richter, O.M., Pfitzner, U., Odenwald, A., Ludwig, B., Michel, H. and Mantele, W. (1998) *Biochemistry* 37, 7390–7399.
- [11] Behr, J., Hellwig, P., Mantele, W. and Michel, H. (1998) *Biochemistry* 37, 7400–7406.
- [12] Hellwig, P., Soulimane, T., Buse, G. and Mantele, W. (1999) *FEBS Lett.* 458, 83–86.
- [13] Lübben, M. and Gerwert, K. (1996) *FEBS Lett.* 397, 303–307.
- [14] Lübben, M., Prutsch, A., Mamat, B. and Gerwert, K. (1999) *Biochemistry* 38, 2048–2056.
- [15] Yamazaki, Y., Kandori, H. and Mogi, T. (1999) *J. Biochem. Tokyo* 126, 194–199.
- [16] Heitbrink, D., Sigurdson, H., Brzezinski, P. and Heberle, J. (2001) submitted.
- [17] Harrick, N.J. (1967) *Internal Reflection Spectroscopy*, John Wiley and Sons, Inc., New York.
- [18] Heberle, J. and Zscherp, C. (1996) *Appl. Spectrosc.* 50, 588–596.
- [19] Mitchell, D.M. and Gennis, R.B. (1995) *FEBS Lett.* 368, 148–150.
- [20] Soulimane, T. and Buse, G. (1995) *Eur. J. Biochem.* 227, 588–595.
- [21] Brandt, U., Schagger, H. and von Jagow, G. (1989) *Eur. J. Biochem.* 182, 705–711.
- [22] Kodama, M., Miyata, T. and Takaichi, Y. (1993) *Biochim. Biophys. Acta* 1169, 90–97.
- [23] Zscherp, C. and Heberle, J. (1997) *J. Phys. Chem. B* 101, 10542–10547.
- [24] Rigaud, J.L., Mosser, G., Lacapere, J.J., Olofsson, A., Levy, D. and Ranck, J.L. (1997) *J. Struct. Biol.* 118, 226–235.
- [25] Rigaud, J.L., Levy, D., Mosser, G. and Lambert, O. (1998) *Eur. Biophys. J.* 27, 305–319.
- [26] Verkhovskaya, M.L., Garcia-Horsman, A., Puustinen, A., Rigaud, J.L., Morgan, J.E., Verkhovsky, M.I. and Wikström, M. (1997) *Proc. Natl. Acad. Sci. USA* 94, 10128–10131.
- [27] Jasaitis, A., Verkhovsky, M.I., Morgan, J.E., Verkhovskaya, M.L. and Wikstrom, M. (1999) *Biochemistry* 38, 2697–2706.
- [28] Vanneste, W.H. (1966) *Biochemistry* 5, 838–848.
- [29] Lemon, D.D., Calhoun, M.W., Gennis, R.B. and Woodruff, W.H. (1993) *Biochemistry* 32, 11953–11956.
- [30] Einarsdottir, O., Dyer, R.B., Lemon, D.D., Killough, P.M., Hubig, S.M., Atherton, S.J., Lopez-Garriga, J.J., Palmer, G. and Woodruff, W.H. (1993) *Biochemistry* 32, 12013–12024.
- [31] Lee, H.M., Das, T.K., Rousseau, D.L., Mills, D., Ferguson-Miller, S. and Gennis, R.B. (2000) *Biochemistry* 39, 2989–2996.
- [32] Heibel, G.E., Hildebrandt, P., Ludwig, B., Steinrucke, P., Soulimane, T. and Buse, G. (1993) *Biochemistry* 32, 10866–10877.